Applicability of OLCI Sentinel-3 RED and NIR bands for chlorophyll-a retrieval in complex waters: Guanabara Bay case study

by

Márcio Vinícius Costa Lopes

A thesis submitted in partial fulfillment of the requirements for the degree of Master of

Science in Meteorology

Department of Meteorology

Federal University of Rio de Janeiro

2023

Applicability of OLCI Sentinel-3 RED and NIR bands for chlorophyll-a retrieval in complex waters: Guanabara Bay case study

Márcio Vinícius Costa Lopes

A thesis submitted in partial fulfillment of the requirements for the degree of Master of Science in Meteorology

Advisor: Dr. Mauro Cirano

Co-advisor: Dra. Priscila K. Lange

Rio de Janeiro, RJ

2023

Abstract

Due to its high sensitivity to environmental changes, phytoplankton is considered a great biological indicator for the analysis of large-scale seasonal events and the evaluation of processes associated with natural and anthropogenic eutrophication. In this context, the present work utilizes OLCI Sentinel-3 RED-NIR bands for the parametrization of chlorophyll-a algorithms that could support phytoplankton bloom monitoring and water quality assessment at Guanabara Bay, a particularly important estuarine environment located in the state of Rio de Janeiro, Brazil. The RED-NIR channels were processed using the ACOLITE atmospheric correction method which is indicated for the study of turbid waters. Six algorithms showed a high level of correlation with the *in situ* chlorophyll-a data (R^2 between 0.72 and 0.84) and the ratio Rrs709/Rrs674 was demonstrated to be a good proxy for phytoplankton distribution on a distinctive summer bloom situation. The results point to the sensitivity of Guanabara Bay's ecosystem to seasonal variability and indicate the suitability and importance of applying Sentinel-3 data on a continuous phytoplankton monitoring program.

Keywords: Remote sensing, Ecosystem health, Guanabara Bay, OLCI Sentinel-3, Chlorophyll-a.

Acknowledgements

I would like to thank my family for all the support throughout these years, my mentors for the opportunity to develop this work and CAPES (*Coordenação de Aperfeiçoamento de Pessoal de Nível Superior*) for the financial subsidy.

List of Figures

List of Tables

Table of Contents

1. Introduction

Remote sensing techniques find applications in several areas of geosciences, leading to numerous advantages such as the possibility of studying the dynamics of the different components of the biosphere by obtaining data frequently (Rustamov et al., 2018). In marine sciences, many works have employed orbital sensors to investigate the optical properties of water, with results being used for the study of primary production and applied to water quality monitoring (Yang et al., 2022). These investigations are of great social/ecological value and can provide information for coastal resources management (Klemas et al., 2011).

The observed spectral properties of a water target are influenced by all optically active constituents (OACs) found in the upper layers of the water column (Figure 1). This feature represents a challenge for the remote sensing study of marine coastal ecosystems because in these environments the non-biogenic OACs (colored dissolved organic matter and inorganic particulate matter) significantly influence water's reflectance profiles (Kirk, 1994; O'Reilly et al., 1998). These constituents absorb a significant fraction of the electromagnetic radiation on the blue range and in coastal waters they generally do not show a good correlation with phytoplankton variation (Gitelson et al., 2007). For this reason, many of the "blue and green based" satellite algorithms for chlorophyll-a retrieval (that are generally suited for oceanic waters) commonly fail to generate good representations of the phytoplankton biomass distribution in coastal areas such as embayments and estuaries (Ha et al., 2017).

Consequently, many authors have applied the strategy of developing algorithms based on the red (RED) and near infrared (NIR) channels (Koponen et al., 2006; Gurlin et al. 2011; Pirasteh et al., 2020). This range of the spectrum represents chlorophyll fluorescence (that is a function of chlorophyll concentration and phytoplankton taxonomy/physiological state), chlorophyll second absorption maximum

and also particulate backscattering properties, whereas the observed contribution of the spectral signatures of OACs that are not derived from phytoplankton is significantly reduced (Gitelson, 1992; Mollaee, 2018; IOCCG, 2021). Secondly, although uncertainties from atmospheric correction methods may still represent a source of error for all types of chlorophyll algorithms, the interference of the atmosphere on the signal of the RED band is considerably smaller compared to that observed in the blue-green range (Wang et al., 2012).

Therefore, many formulations and indexes derived from RED-NIR bands (such as the Normalized Difference Chlorophyll Index - NDCI) have been utilized for estimating phytoplankton biomass in complex waters (Gower et al., 2008; Mishra and Mishra, 2012), while atmospheric correction methods like ACOLITE (which was specifically developed for water applications) have shown improved results in deriving surface reflectance data for RED and RED-edge bands during phytoplankton blooms (Vanhellemont and Ruddick, 2021).
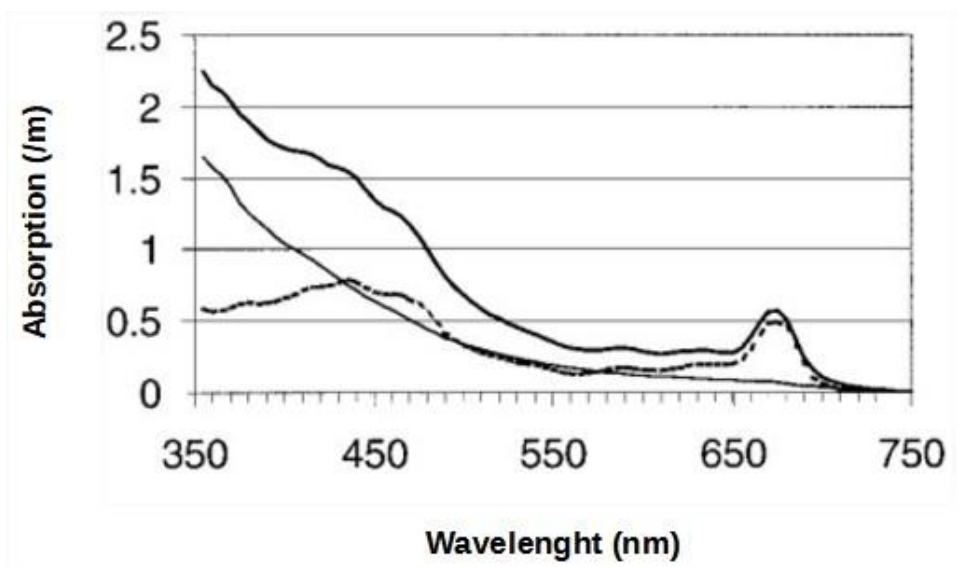
Figure 1: Electromagnetic radiation absorption spectrum of total particulates (upper, thick solid curve) and its components arising from tripton (lower, thin solid curve) and phytoplankton (dashed curve), in a near-shore coastal water sample. An exponential decay can be observed on the lower solid curve while increasing wavelength, which indicates a smaller contribution of tripton on water's spectral properties in the RED-NIR range. Source: **Ruddick et al. (2001)**.

Within today's available orbital sensors, the Ocean and Land Color Instrument (OLCI) from the Sentinel-3 program represents one of the best alternatives for phytoplankton biomass estimates because it features 4 channels on the RED-NIR region, which were specially designed to support chlorophyll-a retrievals (EUMETSAT, 2018). Furthermore, the good spatial (300 m) and temporal resolution (approx. 2 days) of Sentinel 3 satellites (S3A and S3B) also reinforce their suitability for water quality and marine ecological studies, including the monitoring of inland waters (Rodrigues et al., 2022) and the investigation of regions with high dynamic variability (Liu et al., 2021).

Contrasting the numerous benefits that remote sensing analyzes bring for the comprehension of biochemical dynamics of aquatic environments, the number of scientific publications that have employed satellite sensors for the study of marine regions along Brazil's coastline is still very limited (Giannini et al., 2013; Silva and Garcia, 2021). In Guanabara Bay (a socially and economically important estuarine ecosystem located in the state of Rio de Janeiro, Brazil), many papers have focused on the classical methodology to investigate water quality indexes and phytoplankton taxonomy (Villac and Tenenbaum, 2010; Santos, 2015), whereas just a few have utilized remote sensing techniques for chlorophyll-a estimates (Oliveira et al., 2016; Tran et al., 2023) or water mass classification (Soares et al., 2017). Therefore, the potential of remote sensing analysis for estimating phytoplankton biomass in Guanabara Bay remains relatively unexplored.

Aforesaid, supported by a dataset of chlorophyll-a concentrations obtained in Guanabara Bay, this study has applied ACOLITE-derived surface reflectance data from OLCI/Sentinel-3 RED and NIR bands for the parametrization of empirical chlorophyll-a algorithms. This class of algorithms has the advantage of simplicity over analytical and semi-analytical models because they do not require quantitative

information about water's intrinsic optical properties (i.e total absorption and backscattering coefficients) whilst they can still accomplish significantly better results than the commonly available satellite built-in chlorophyll-a products (Mollaee, 2018). Although a challenge for coastal waters, the obtention of more accurate remote sensing chlorophyll-a estimates provides the opportunity to generate more realistic biomass distribution maps and also to develop a satellite chlorophyll-a time series, which can be used for environmental monitoring and climatological evaluation respectively. The generated algorithms' statistical metrics were therefore evaluated and compared, while a March 2022 phytoplankton bloom event was investigated. The influence of the sea surface temperature (SST) on the phytoplankton distribution in Guanabara Bay has been briefly discussed.

2. Methods

2.1. Study area

Guanabara Bay is an estuarine environment located on the southeastern coast of Brazil, centered at 22°50' S and 43°10' W, with a total area of approximately 384 km² and depths ranging from a few meters to up to 40 m (Figure 2) (Kjerfve et al., 1997). On its surroundings there are 15 municipalities, including the city of Rio de Janeiro, which has a population of around 6.2 million inhabitants, according to the 2022 IBGE (Brazilian Institute of Geography and Statistics) census (IBGE, 2023). The bay's drainage basin has an area of approximately 4080 km² and is composed of 55 rivers that, together, contribute with an annual average water discharge of about 200 m³/s (SEA/UEPSAM, 2016).

Located in a region with a humid tropical climate, Guanabara Bay is

classified as a positive estuary with a circulation regime dominated by tidal influence (primarily semidiurnal regime) and, to a lesser extent, by density gradients (Sampaio, 2003). The local circulation is also influenced by cold fronts generally associated with winds with speeds often greater than 10 m/s, and by coastal trapped waves which affect the sub inertial circulation next to the bay's exit and on the adjacent continental shelf (Kjerfve et al., 1997; Pita, 2019).

Due to problems associated with the implementation of industrial activities and disorderly urban growth in its vicinity, it has been possible to observe a considerable intensification of the eutrophication phenomenon on Guanabara Bay's waters (specially on its western section) (Mayr et al., 1989; Hatherly, 2013; Cruz, 2016). This problem is a direct result of the aggravation of anthropogenic pollution (marine and terrigenous) and can be perceived by a noticeable reduction of the bay's water quality indicators (Lima, 2006). This scenario represents a threat to Guanabara Bay's ecosystem and, along with a higher probability of peaks on the Biochemical Oxygen Demand (BOD) (which is associated with several reported "fish kill" events), the increase of heavy metals' discharge such as lead and chromium from industrial effluents is also a factor of concern (Lima, 2006; SEA/UEPSAM, 2016).

Lastly, it is also important to mention that Guanabara Bay and all its adjacent regions are characterized by the existence of different social actors with often divergent interests, a fact that becomes especially critical when is considered that around 6 thousand families depend on fishing activity in Guanabara Bay as a source of income for their subsistence (Fistarol et al., 2015).
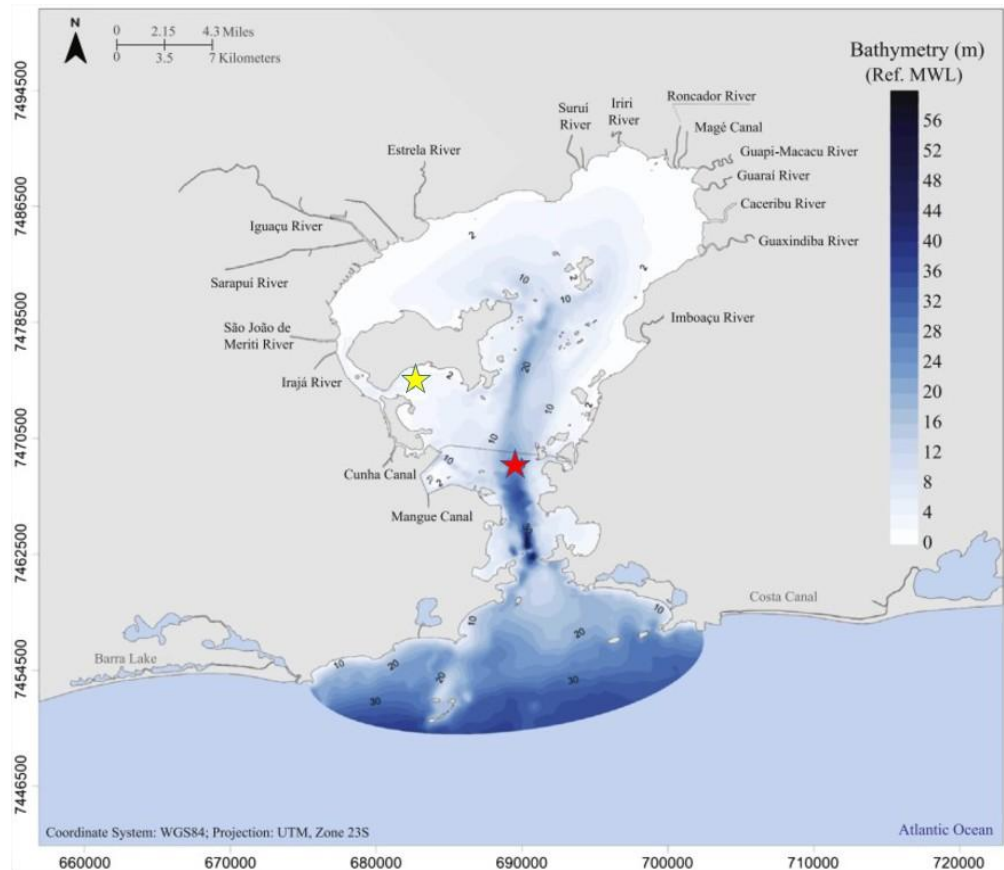
Figure 2: Guanabara Bay and the main rivers that compose its drainage basin. The bathymetry is shown as blue-scaled shades. The approximate position of the sampling points, station A (-22.8253, -43,2216) and station B (-22.8767, -43.1578), are shown as a yellow and a red star, respectively. Source: Andrade (2018). Adapted by Fries et al. (2018).

2.2. *In-situ* chlorophyll-a data

The set of *in-situ* chlorophyll-a data used to parameterize the algorithms consists of 19 concentration values obtained by the analysis of water samples collected in two specific points (stations A and B, Figure 2) in Guanabara Bay between the years of 2017 and 2018. These 19 values were selected from a dataset with 244 values and refer to sampling dates with Sentinel-3 cloud-free imagery match-ups. All sampling campaigns and chlorophyll analysis were carried out by the Laboratory of Marine Phytoplankton (Department of Marine Biology, Institute of Biology, Federal University of Rio de Janeiro) coordinated by Prof. Dr. Paulo Sérgio

Salomon, and the analysis results were kindly provided for this study. Water samples were collected in duplicates, kept hidden from the light and filtered in the laboratory on the same day (using Whatman GF/F (47 mm) filters). For pigment extraction, GF/F filters were dipped in a centrifuge tube containing 5.4 ml of 100% acetone and left in the dark at 4 °C for a 12 hours extraction. Following extraction, the tubes were centrifuged for 5 min at 3500 rpm. The analysis procedure used to determine the concentration of chlorophyll-a on the samples was based on the spectrofluorimetric method and is fully described in Tenório et al. (2005).

2.3. Satellite data processing and fundamentals of remote sensing

Based on the sampling dates (exact match) of the *in-situ* chlorophyll data, a total of fifteen cloud free Sentinel-3A OLCI level-1[1] Full Resolution images were obtained from EUMETSAT (European Organization for the Exploitation of Meteorological Satellites) Data Centre (https://www.eumetsat.int/eumetsat-data-centre). All scenes were atmospherically corrected using the ACOLITE atmospheric correction method (Vanhellemont and Ruddick, 2016) which is based on the dark spectrum fitting (DSF) algorithm (Vanhellemont, 2019). This method was originally developed to process LANDSAT and Sentinel-2 images (with focus on the study of turbid coastal waters) and it was further adapted to process Sentinel-3 data (Vanhellemont and Ruddick, 2021). The procedure converts Top of the Atmosphere (TOA) radiance to remote sensing reflectance (R_{rs}) for sixteen OLCI's bands (ranging from 0.4 to 1.02 μm) and it was chosen over the baseline (Bright Pixel Atmospheric Correction - BPAC) and the alternative (Case 2 Regional Coast Color - C2RCC)

---

[1] Level 1 data consists of georeferenced, quality controlled and pixel classified data (land, water, coastline, etc) of radiometrically calibrated TOA radiance.

Sentinel-3 atmospheric correction methods (EUMETSAT, 2018). The reason for this selection was the negative reflectance values that often result from the use of BPAC for the remote sensing study of complex waters (Moses et al., 2009a) and the well reported[2] underestimates of red and red-edge reflectances associated with the application of C2RCC (Moses et al., 2009b). For each of the fifteen scenes, after the ACOLITE processing was complete, the software Sentinel Application Platform (SNAP) was used to extract the R_{rs} values from the pixels corresponding to the sampling points (Stations A and B).

Equation 1 shows the relationship between R_{rs} and two inherent optical properties (IOPs) namely, total absorption (a(λ) and backscattering coefficients ($b_b(\lambda)$):

$$R(\lambda) \propto \gamma \frac{b_b(\lambda)}{a(\lambda) + b_b(\lambda)} \tag{1}$$

The observed model is a semi analytic approximation derived from the radiative energy transfer equation and Y (gamma) is dependent on the geometry of the light field emerging from water (Gordon et al., 1988; Gitelson et al., 2007). For the remote sensing analysis, the importance of the spatial resolution parameter is evidenced by the fact that both a(λ) and $b_b(\lambda)$ can be decomposed in terms of the contributions of the individual OACs present on water (ie. chlorophyll, CDOM and tripton) plus the contribution of water itself. Water's absorption and backscattering coefficients are not expected to vary significantly in space but those related to OACs can vary greatly because of different type/size of inorganic particulate matter and also possible biological and physiological variations on the phytoplankton community (Gitelson et al., 2007; IOCCG,

---

[2] This issue, as reported by Binding et al. (2011) is a special problem on the investigation of phytoplankton blooms and is associated with the non representation of chlorophyll-a fluorescence features.

2021). Another determinant parameter for the remote sensing study is the choice of which bands will be applied associated with the spectral resolution of these specific bands. As previously mentioned (Section 1) the different OACs have distinct spectral signatures which is the result of a varying absorption/backscattering behavior considering the different wavelengths. CDOM for example strongly absorbs radiation on the blue region whilst inorganic particulate matter and phytoplankton can significantly influence water's backscattering on the NIR region (Zeng and Binding, 2019). Therefore the success of the utilization of R_{rs} with the purpose of evaluating one specific OAC by means of a empirical relationship depends, among other factors, on the minimization of the impact that other OACs may have on R_{rs} and on an adequate spatial resolution that will minimize errors associated with the spatial variability of the target OAC.

2.4. Sentinel-3 bands and formulations

The algorithms for chlorophyll-a retrieval were parameterized based on four different OLCI/Sentinel-3 bands. The main characteristics of these bands and their specification (which are related with features that are present in chlorophyll-a absorption spectra) are shown in Table 1. The formulations applied to develop the algorithms are shown in Table 2. Expressions (d), (f) and (h) are the normalized versions of the simple band ratios presented in expressions (c), (e) and (g), respectively. From Table 2 it's noted, for example, that the formulation Rrs709/Rrs681 can be interpreted as the ratio between the Chlorophyll fluorescence peak and the signal relative to chlorophyll fluorescence baseline.

Table 1: Characteristics of the OLCI/Sentinel-3 bands used in the chlorophyll-a algorithms. Source:EUMETSAT (2018).

Band	Central wavelength (nm)	Band width (nm)	Specification	Spatial resolution (m)
Oa08	665	660-670	Red, 2º chlorophyll absorption maximum	300
Oa09	673.75	670-677.5	For improved fluorescence retrieval	
Oa10	681.25	677.5-685	Red edge, chlorophyll fluorescence peak	
Oa11	708.75	703.75-713.75	Red edge transition, chlorophyll fluorescence baseline	

Table 2: Applied formulations based on OLCI/Sentinel-3 RED and NIR bands. References: Gitelson et al. (2007), Gurlin et al. (2011), Mishra and Mishra (2012) and Lins et al. (2017).

Formulation			
$Rrs681/Rrs665$	(a)	$Rrs709/Rrs674$	(e)
$Rrs674/Rrs665$	(b)	$(Rrs709-Rrs674)/(Rrs709+Rrs674)$	(f)
$Rrs709/Rrs665$	(c)	$Rrs709/Rrs681$	(g)
$(Rrs709-Rrs665)/(Rrs709+Rrs665)$[3]	(d)	$(Rrs709-Rrs681)/(Rrs709+Rrs681)$	(h)

---

[3] NDCI. Mishra and Mishra (2012)

2.5. Statistical analysis and investigation of a phytoplankton bloom event

In this study, the algorithms were statistically evaluated by the application of three different metrics: Coefficient of determination (R^2), mean absolute error (MAE, Eq. (2)) and root mean square error (RMSE, Eq. (3)). MAE and RMS were calculated as follows[4]:

$$\text{MAE:} \quad \frac{1}{N} \sum_{i=1}^{N} |x_{f,i} - x_{o,i}| \tag{2}$$

$$\text{RMSE:} \quad \sqrt{\frac{1}{N} \sum_{i=1}^{N} \left(x_{f,i} - x_{o,i}\right)^2} \tag{3}$$

Based on the statistical results, SNAP 8.0 and QGis 3.30.2 softwares were utilized to create images of a specific bloom event that occurred in Guanabara Bay in the summer of 2022. This event is here represented by four cloud-free Sentinel-3A OLCI level-1 Full Resolution scenes which were downloaded and processed in a similar way as described in Section 2.2. To uphold the discussion and to outline the relationship between Sea Surface Temperature (SST) and the occurrence of blooms in Guanabara Bay, a one year screen of the *in-situ* chlorophyll-a time series was compared to SST data derived from the NASA MODIS program (Vermote et al., 2015).

---

[4] N is the number of values; $X_{f,i}$ is the value obtained from the regression line and $X_{o,i}$ is the *in-situ* value.

3. Results and discussion

3.1. *In-situ* chlorophyll-a data variability

The temporal variability considering the complete chlorophyll-a *in-situ* dataset (244 concentration values) and a screening of the 2017-2018 period is presented in Figure 3. The summary statistics considering the entire chlorophyll concentration data can be assessed in Table 3 while the descriptive statistics of the in-situ chlorophyll subset used to parametrize the algorithms is shown in Table 4.

Table 3: Summary statistics of the complete chlorophyll-a *in-situ* dataset. Dry season corresponds to the period from May to October whereas the rainy season corresponds from November to April.

Seasonality	Station	No. of values	Min. (µg /L)	Max. (µg /L)	Mean (µg /L)	Std (µg /L)	Frequency > 100µg /L
Dry season	A	54	13.77	183.61	75.02	49.74	17
	B	75	1.16	158.44	22.42	24.21	1
	A+B	129	1.16	183.61	44.44	45.19	18
Rainy season	A	44	10.11	398.42	94.46	82.39	17
	B	71	2.63	266.49	44.31	41.70	6
	A+B	115	2.63	398.42	63.50	65.02	23

Table 4: Summary statistics of the chlorophyll-a *in-situ* data used to develop the algorithms.

Station	No. of values	Min. (µg /L)	Max. (µg /L)	Mean (µg /L)	Std (µg /L)
A	8	48.01	177.93	116.94	42.27
B	11	8.35	144.62	42.24	39.38
A+B	19	8.35	177.93	73.69	54.70

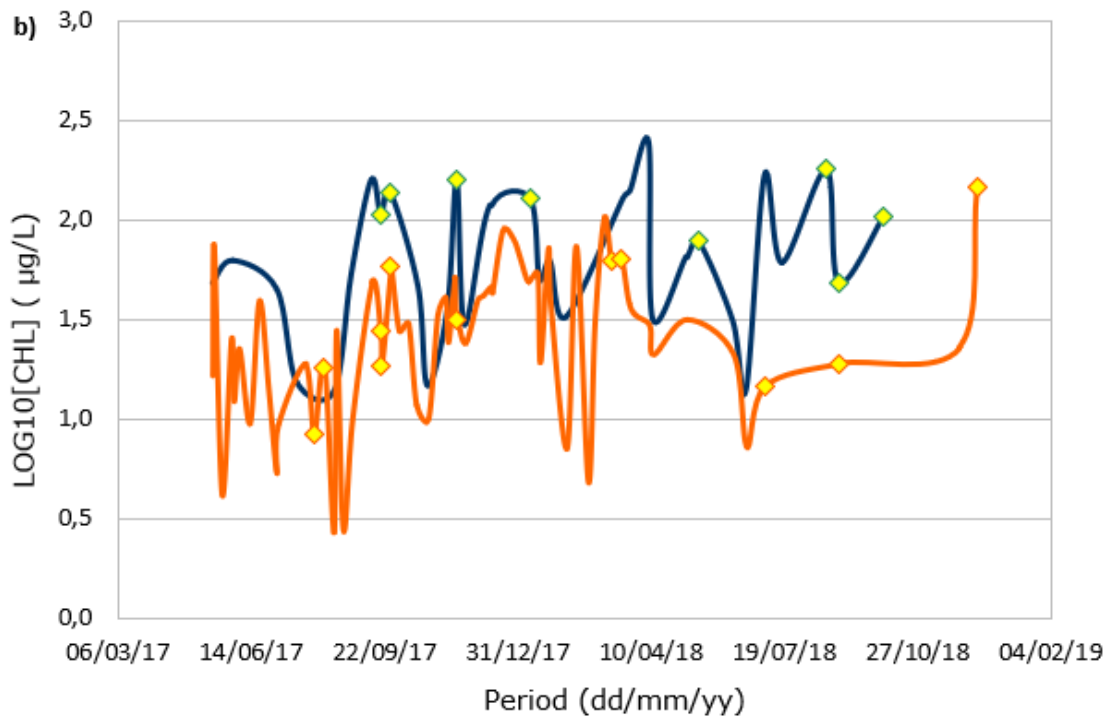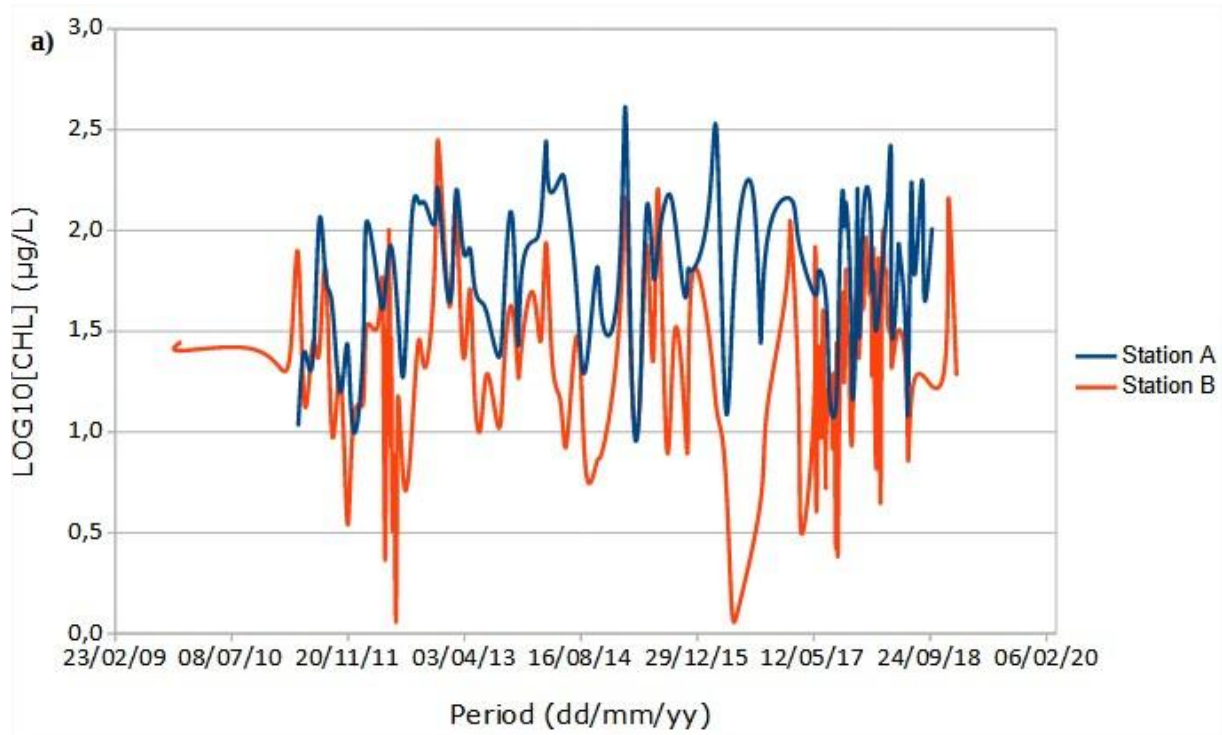Figure 3: Temporal variability of *in-situ* chlorophyll-a concentrations at the two sampling stations in Guanabara Bay considering: a) The whole dataset; b) The data obtained between 2017-2018 (yellow markers indicate the dates with satellite match up). Data provided by the Laboratory of Marine Phytoplankton (Department of Marine Biology, Institute of Biology, Federal University of Rio de Janeiro).

On average, chlorophyll-a concentrations are higher at Station A than those observed at Station B (Tables 3 and 4; Fig. 3). This can be interpreted considering the combined result of the oceanic influence (which is greater at Station B) and the terrigenous influence (which is more pronounced at Station A). The mean chlorophyll concentration and the standard deviation (STD) are higher in the rainy season for both stations, with STD being noticeably higher at Station A (which indicates a more accentuated chlorophyll variability on this point - Table 3). The observed summary statistics of the *in-situ* chlorophyll-a subset used for algorithm development (Table 4) shows that even though it was only possible to obtain Sentinel-3 match-up for 7.8% of the data (19 of 244 concentration values) the mean and also the variation amplitude of this values are quite representative of the complete dataset (Table 4 vs Table 3).

The statistical results presented in this section highlight the seasonal variability of chlorophyll-a (and therefore of phytoplankton) in Guanabara Bay and are in good agreement with previous studies (Table 5). Oliveira et al., 2016 for exemple, found that the chlorophyll-a standard deviation values were higher on the rainy season (in comparison to that of the dry season) considering five different sectors of the bay. Their results and the results of Santos, 2015 also show that the chlorophyll-a variability is lower on the sections of the bay that have more oceanic influence (bay's entrance and central channel).

As mentioned in section 2.2, it is important to note that the chlorophyll-a *in-situ* dataset utilized in this work has been provided by the Laboratory of Marine Phytoplankton (Department of Marine Biology, Institute of Biology, Federal University of Rio de Janeiro) coordinated by Prof. Dr. Paulo Sérgio Salomon and Dr. Márcio Tenório and it has not not been published elsewhere.

Table 5: Previous investigations of chlorophyll-a distribution in Guanabara Bay. Source: Santos (2015); Oliveira et al. (2016); Gregoracci et al. (2012); Paranhos et al. (2001) and Mayr et al. (1989).

Seasonality	Sections/points	N	Mean (µg /L)	Min. (µg /L)	Max. (µg /L)	STD (µg /L)	Reference
Full period	East sector, entrance and central channel	—	—	4.0	28.6	—	Mayr et al. (1989)
	West sector	—	—	28.96	148.8	—	
	Urca Beach	46	13.33	0	58.24	—	Paranhos et al. (2001)
	Ramos Beach		118.2	7.26	483.5	—	
	Bay's entrance	—	30.84	—	—	29.47	Gregoracci et al. (2012)
	Rio-Niteroi bridge	—	46.29	—	—	42.63	
	Ilha do Governador	—	171.28	—	—	143.96	
Dry season	Bay's entrance	22	11.43	2.0	37.0	7.83	Santos (2015)
	Ilha do Governador	19	25	3.34	200	43.85	
	Central section	17	27.42	74.80	164	19.60	
	Northeast section	21	52.55	4.20	162.20	44.54	
	Northwest section	29	78.51	6.20	324	73.32	
Rainy season	Bay's entrance	14	24.83	2.60	126	31.61	
	Ilha do Governador	14	122	4.90	279	93.51	
	Central section	16	85.4	1.80	213.0	69.41	
	Northeast section	10	76.61	17.0	195.0	60.80	
	Northwest section	18	86.77	8.20	211	61.59	
Dry season	Bay's entrance	76	14.8	1.4	57.0	14.4	Oliveira et al. (2016)
	Central channel	49	32.7	2.6	96.0	25.8	
	Ilha de Paquetá	37	39.2	6.0	142.8	30.3	
	Northeast section	50	71.4	11.1	371.0	70.5	
	West sector	100	86.1	1.7	736.4	95.2	
Rainy season	Bay's entrance	62	29.1	1.0	188.1	33.3	
	Central channel	39	40.9	3.4	140.1	29.2	
	Ilha de Paqueta	28	86.4	6.8	559.9	118.3	
	Northeast section	44	66.1	14.1	829.1	120.4	
	West sector	85	141.6	1.4	974.0	177.9	

3.2. Model parametrization and statistical analysis

The performances of the RED-NIR chlorophyll algorithms were overall different for each of the eight models analyzed (Figure 4, Table 6). Considering the wide range of the applied *in-situ* chlorophyll-a concentrations (8.35 to 177.93 µg /L), two models (Rrs681/Rrs665 and Rrs674/Rrs665) did not present satisfactory performances while the other six models exhibited good or very good linear correlations, with R^2 values varying between 0.72 and 0.84 (Table 6).

Table 6: Equations and statistical metrics of the algorithms[5].

Model	R^2	RMSE (µg /L)	MAE (µg /L)	Equation
Rrs681/Rrs665	0.01	—	—	—
Rrs673/Rrs665	0.02	—	—	—
Rrs709/Rrs665	0.72	28.10	21.52	122.774*(Rrs709/Rrs665) -89.619
NDCI	0.72	28.05	21.38	328.423*(NDCI)+37.000
Rrs709/Rrs674	0.81	23.03	18.21	152.006*(Rrs709/Rrs674) -111.276
(Rrs709-Rrs674)/ (Rrs709+Rrs674)	0.80	23.77	18.49	369.295*(x)+44.302
Rrs709/Rrs681	0.84	21.06	18.13	198.958*(Rrs709/Rrs681) -131.141
(Rrs709-Rrs681)/ (Rrs709+Rrs681)	0.80	23.68	20.27	395.283*(x)+73.689

---

[5] Model bias was equal to zero for all formulations.
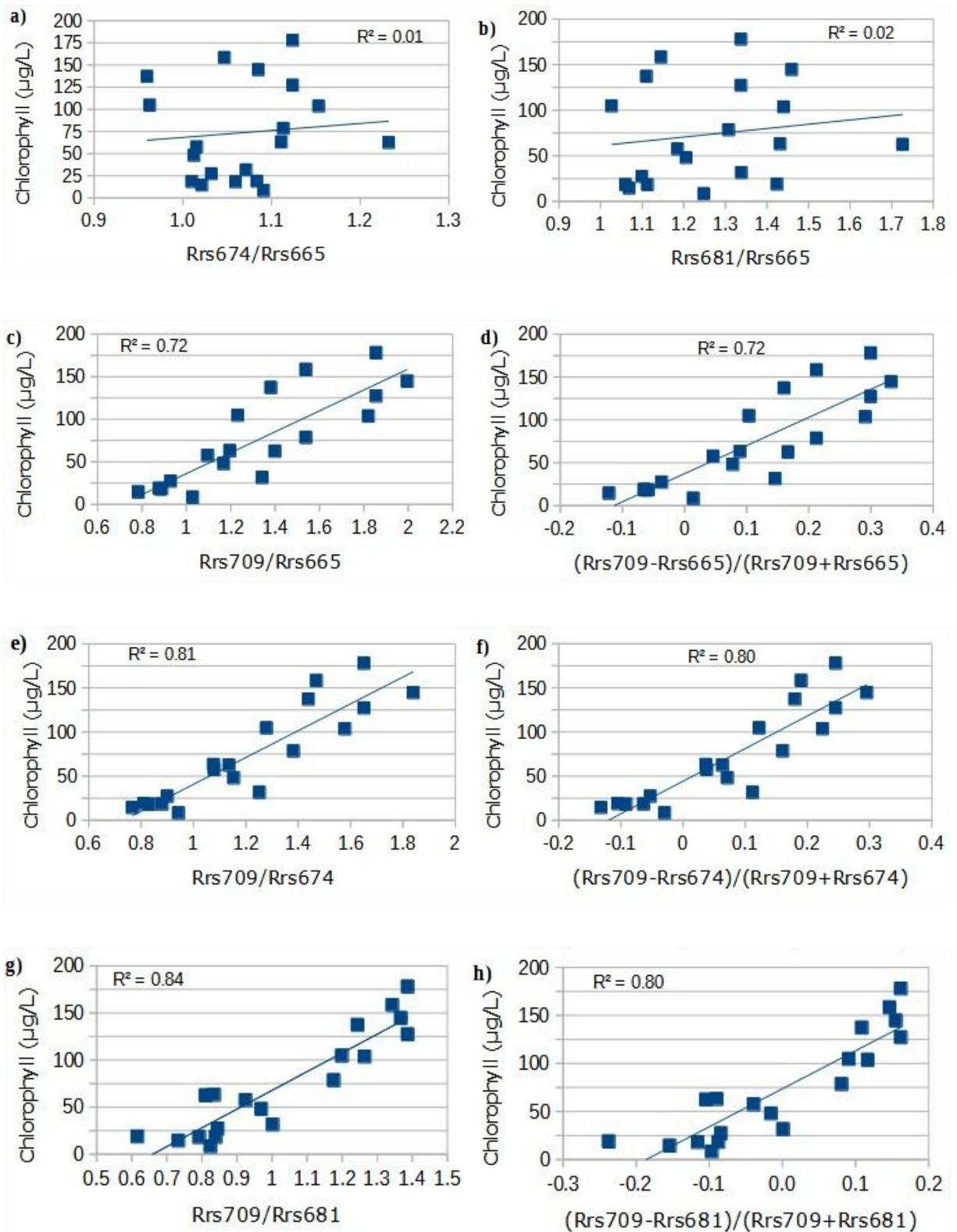
Figure 4: Relationship between RED-NIR ratios and *in-situ* chlorophyll-a concentrations in the models based on the following band ratios:(a)Rrs681/Rrs665, (b)Rrs674/Rrs665, (c)Rrs709/Rrs665, (d)(Rrs709-Rrs665)/(Rrs709+Rrs665), (e)Rrs709/Rrs674, (f)(Rrs709-Rrs674)/(Rrs709+Rrs674), (g)Rrs709/Rrs681 and (h) (Rrs709-Rrs681)/(Rrs709+Rrs681).

The band ratio Rrs709/Rrs681 showed the lowest RMSE value (21.06 µg /L), possibly due to the better fit obtained by this model on the chlorophyll-a range above 75 µg /L (Figure 4d; Table 6). Comparatively, the band ratio Rrs709/Rrs674 and its normalized difference formulation (Rrs709-Rrs674)/(Rrs709+Rrs674) displayed a slightly higher RMSE (23.03 and 23.77 µg /L respectively) but a better fit for moderate chlorophyll concentrations (Figure 4e and 4f). No significant correlation was found when applying the ratio Rrs681/Rrs674 (R^2=0.03) and the "blue and green" ratios (Rrs560/Rrs443 and Rrs560/Rrs490 - R^2 < 0.1) (data not shown).

A hybrid model (Figure 5) can be first analyzed by applying the Rrs709/Rrs674 ratio for chlorophyll-a concentrations below or equal 75 µg /L and the ratio Rrs709/Rrs681 for concentrations above this limit. With n=18 the observed linear expression ([Chl]= 246.55x + 197.18; R^2=0.87) shows a MAE and RMSE of 13.38 µg /L and 19.54 µg /L respectively, which points to an even better performance than the associated simple models. Another possibility of an algorithm that would utilize two band ratios for chlorophyll-a retrieval is a switch algorithm based on the expressions [Chl]=152.00*(R_{rs}709/R_{rs}674)-111.27 and [Chl]=198.96*(R_{rs}709/R_{rs}681)-131.14 (Table 6). This class of algorithm has been the main subject for example, of a work published by Smith et al. (2018), where the authors develop a model based on the selection of a blue-green or a Red-NIR model depending on the value of the ratio Rrs708/Rrs665 . As the purpose of the present work is a more broad evaluation of the application of Sentinel-3 Red-NIR bands in Guanabara Bay, this class of algorithms will be subject of further studies.
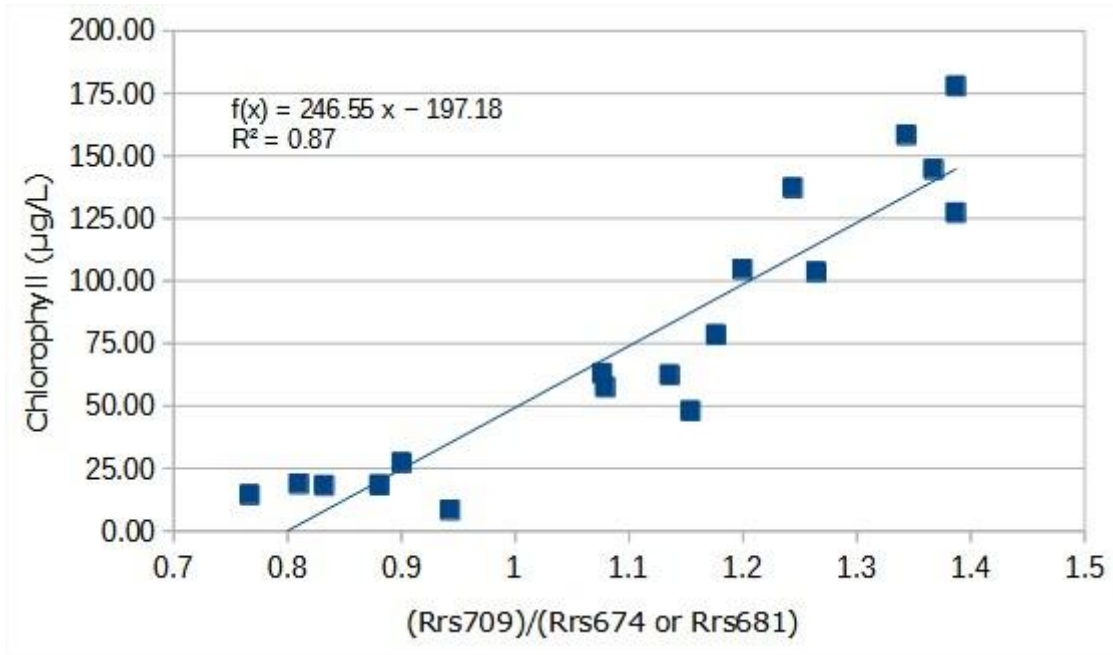
Figure 5: Relationship between RED-NIR ratio and *in-situ* chlorophyll-a concentrations (hybrid model). $R_{rs}709/R_{rs}674$ ratio has been applied for chlorophyll-a concentrations below or equal 75 µg /L whereas $R_{rs}709/R_{rs}681$ has been applied for chlorophyll-a concentrations above this value.

The observed relationship between the *in-situ* chlorophyll-a and the spectral reflectance data (Figures 4c - 4h) indicates an increase of the ratios Rrs709/Rrs681, Rrs709/Rrs674 and Rrs709/Rrs665 as chlorophyll concentrations rise. This behavior is associated with a variation on the shape of the water-leaving RED-NIR reflectance profile and can be interpreted considering the redshift of the red-edge reflectance peak (which is associated with high chlorophyll absorption and high particulate backscattering) (Gilerson et al., 2010; Tal et al. 2013; Lins et al. 2017). As demonstrated by Gitelson, 1992 the red-edge reflectance peak observed on different natural water bodies (that can be interpreted as the merged result of chlorophyll fluorescence and a minimum on the combined absorption profile of phytoplankton and water) can shift from approximately 680 nm to nearly 715 nm exhibiting a correlation coefficient of more than 0.9 with increasing chlorophyll concentration (~5 µg /L - 120 µg /L) (Gitelson, 1992). Similarly, the occurrence of the redshift has been shown to be positively correlated with the ratio Rrs709/Rrs665, when two

25

different phytoplankton species were evaluated individually (Tal et al. 2013).

Despite the overall good statistical performances that were obtained by the RED-NIR algorithms, some of the associated uncertainties can be discussed based on the high level of biological and physicochemical variability of Guanabara Bay water masses (Sampaio, 2003; Lima 2006; Santos, 2015; Andrade, 2018). According to Tao et al., 2013, the ratio of the described red shift varies depending on two water-related optical parameters namely the chlorophyll fluorescence quantum efficiency $\varphi_{(\lambda)}$ and the chlorophyll-specific absorption coefficient $a*_{ph}(\lambda)$ (Tao et al., 2013). These two parameters play a fundamental role in determining waters' intrinsic optical properties (total absorption - $a(\lambda)$ and backscattering - $bb(\lambda)$ coefficients) and their magnitude is highly dependent on biological factors like the phytoplankton physiological state and taxonomic composition (Gitelson et al. 2017; IOCCG, 2021). Therefore, it's observed that a change on the phytoplankton structure (which could be the result of natural or anthropogenic stress) can have a direct impact on both $\varphi_{(\lambda)}$ and $a*_{ph}(\lambda)$ and consequently on the red edge spectral profile of water-leaving reflectance (Gitelson et al, 2007; Gilerson et al. 2010).

Besides the discussed influence of $\varphi_{(\lambda)}$ and $a*_{ph}(\lambda)$ the algorithms are prone to errors related to *in-situ* data acquisition and also the influence of the atmosphere/atmospheric correction method (IOCCG, 2019). A major example of the first issue is the time lapse between satellite overpass and water sampling, which is associated with different scenarios considering the possible situations of the tide cycle. As an exemplification, considering the same time interval between sampling and satellite overpass, a spring tide can theoretically promote a higher variation on the chlorophyll-a concentration in comparison to a neap tide whereas a flood current would promote a different chlorophyll-a variability in relation to an ebb current (oceanic vs continental influence). Nevertheless, performance

results (Table 6) are similar to those obtained by different studies that considered the application of RED and NIR bands (Table 7). Furthermore, the moderate RMSE values observed for six of the eight chlorophyll-a RED-NIR algorithms (21.06 µg/L to 28.10 µg/L) are indicative of their prospectiveness for the identification and monitoring of phytoplankton blooms in Guanabara Bay.

Table 7: Compilation of previous works related to RED-NIR chlorophyll-a algorithms. The observed amounts of total suspended solids in these environments are highly variable, with observed maximum values reaching 61 g/m³ in Munduaú/Manguaba Lagoon (Lins et al. (2017)) and 19.6 g/m³ in the Lake Woods (Binding et al. (2011)) respectively. Publications that have used *in-situ* radiometric data to simulate the satellite bands are indicated by "*".

Study area	Sensor	Formulation	Chl range (µg /L)	N	R^2	Reference
Johor Strait (Singapore)	—	R672/R695	0.5 - 139.4	102	0.68	Gin et al. (2001)
Chesapeake Bay	MERIS*	(1/R665-1/Rrs709) x Rrs754	9.0 – 77.4	44	0.75	Gitelson et al. (2007)
Lake Thai	—	R719/R667	< 200	28	0.87	Jiao et al. (2007)
Azov Sea	MERIS	Rrs709/Rrs665	0.63 – 65.51	18	0.97	Moses et al. (2009b)
Lake Woods	MERIS	MCI [6]	1.90 - 70.50	17	0.72	Binding et al. (2011)
Freemont Lakes	MERIS*	Rrs709/Rrs665	3.97 -100.00	89	0.95	Gurlin et al. (2011)
Mundaú/ Manguaba Lagoon	OLCI*	R709/R681	0.97 - 117.54	72	0.71	Lins et al. (2017)
Funil Reservoir	OLCI*	294,49(NDCI)²+ 119,51(NDCI) +19,688	2.33 - 306.03	29	0.98	Watanabe et al. (2018)
East coast of India	OLCI	MCI	0.50 – 18.00	30	0.84	Shaik et al. (2021)

---

[6] MCI (Maximum Chlorophyll Index) formulation relates to the height of the reflectance peak at 709 nm (Binding et al, 2013).

3.3. Phytoplankton bloom case study

The analysis of four ACOLITE derived Sentinel-3 images of Guanabara Bay from March 2022 (Figure 6) revealed a variation in water color that is indicative of a change in phytoplankton bloom structure and abundance (Reguera et al., 2008; Ahmad et al., 2009; Zhou et al., 2021).
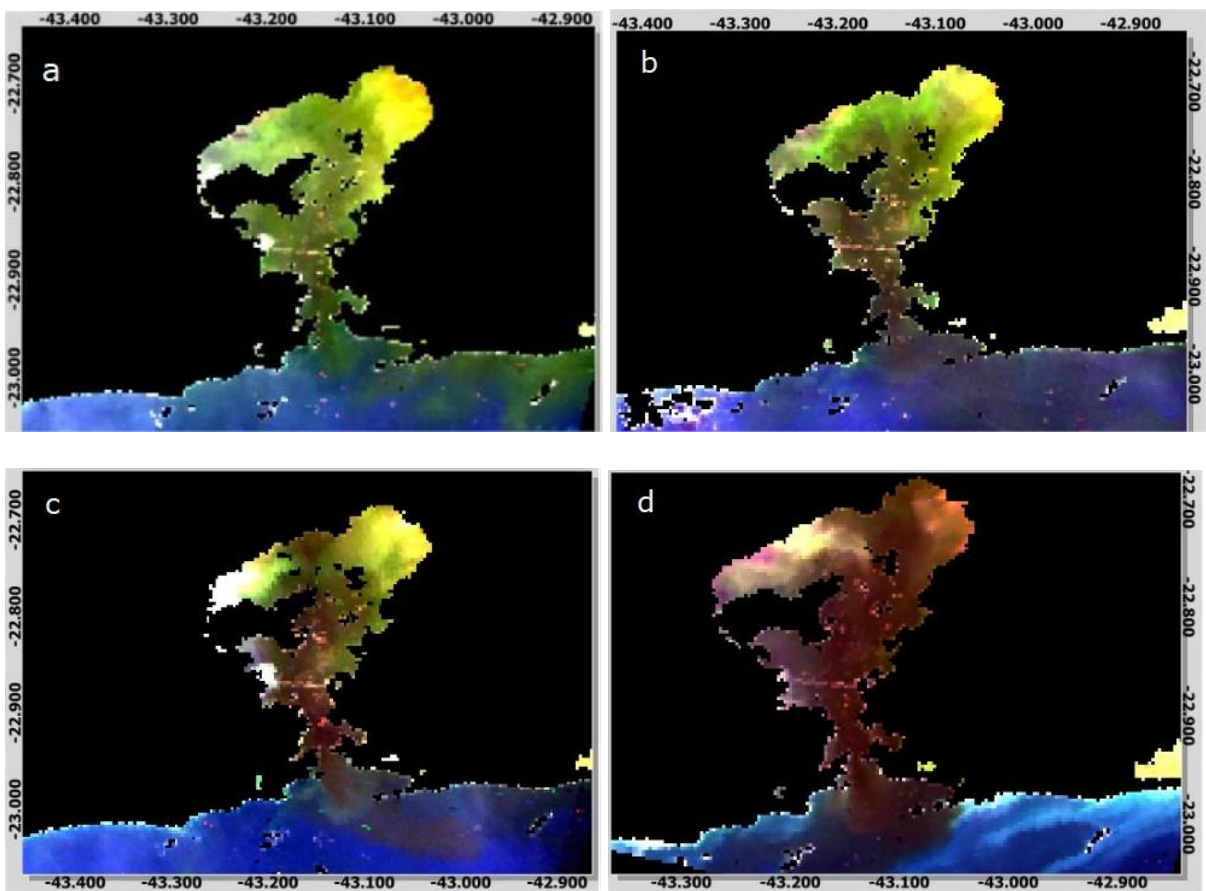
Figure 6: Sentinel-3 RGB images of a summer phytoplankton bloom event in Guanabara Bay. (a) March 5, 2022; (b) March 9, 2022; (c) March 17, 2022; (d) March 24, 2022

The observed bloom was coincident with maximum temperature records reported in Rio de Janeiro in this period, whereby all day maximums were above 30°C (reaching 38,7 °C and 38,6 °C on March, 1 and March, 6 respectively) and no rain precipitation was observed within a

period of 15 days (from February, 22 to March 8), which ranks March, 2022 as the hottest month of march in Rio de Janeiro considering the last eleven years (INMET, 2022). The bloom event is therefore proposed to be associated with the influence exerted by sea surface temperature (SST) on the dynamics and frequency of phytoplankton blooms on inland waters and also on coastal and oceanic environments (Dai et al., 2023). Such association is hereby supported by the noticeable connection between higher MODIS SST values and a more pronounced variability of the chlorophyll-a concentration in Guanabara Bay (Figure 7).
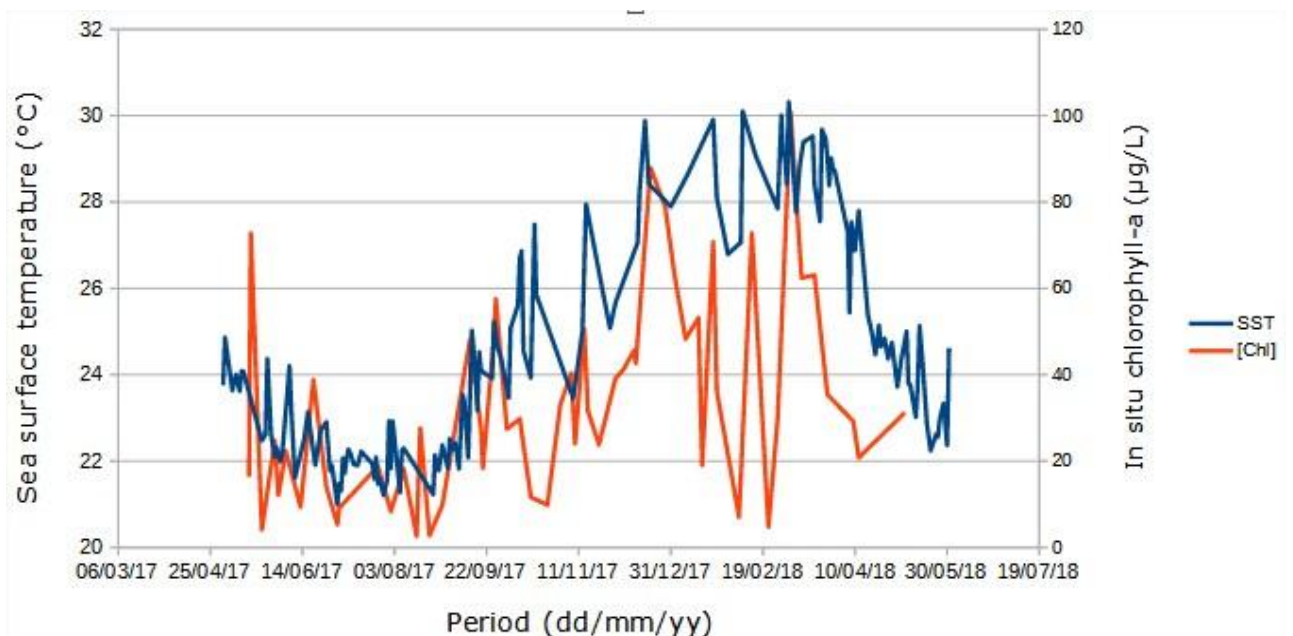
Figure 7: Comparison of the chlorophyll-a variation on Station B (orange line) between May 2017 and May 2018 and MODIS SST time series of a central point (-22.86, -43.16) of Guanabara Bay on the same period (blue line). Modis SST data was utilized because *in-situ* SST data from the SiMCosta program (RJ-3 and RJ-4 buoys - Franz et al. (2021)), was not available for this period.

This scenario suggests that the influence exerted by increased air temperature associated with low wind speeds (possibly driving water column stratification) may be determinant for the dynamics of phytoplankton blooms in Guanabara Bay and this relationship could, especially in the summer, synergize with the eutrophication problem

causing changes in phytoplankton community structure (Figure 6) and peaks in phytoplankton biomass (Figure 7) that could be potentially harmful to the ecosystem balance and to human health (Fries et al. 2019; Rumyantseva et al., 2019).

Given the good statistical performance obtained by the simple band ratio Rrs709/Rrs674 (Section 3.1 - Figure 4e) and its observed tighter fit on the "low" to moderate chlorophyll range (where the relative errors on the chlorophyll estimates could be more impacting), this formulation was applied to represent the phytoplankton distribution patterns of March 17, 2022 (Figure 6c) and March 24 2022 (Figure 6d).

It is observed (Figure 8) that irrespective of the water color change that took place between March 17, 2022 and March 24, 2022 (which indicates a variation on the phytoplankton structure), a consistent qualitative correlation between the ratio Rrs709/Rrs674 and the areas more affected by the bloom is found for both scenes (i.e higher values of the ratio are associated with the areas on Figures 6c and 6d where green or red color are more intense). This result aggregates with the statistical results presented in Section 3.2 (Figure 4e), and is another indicator that the band ratio Rrs709/Rrs674 is representative of chlorophyll-a distribution and it could be utilized for water quality monitoring in Guanabara Bay.
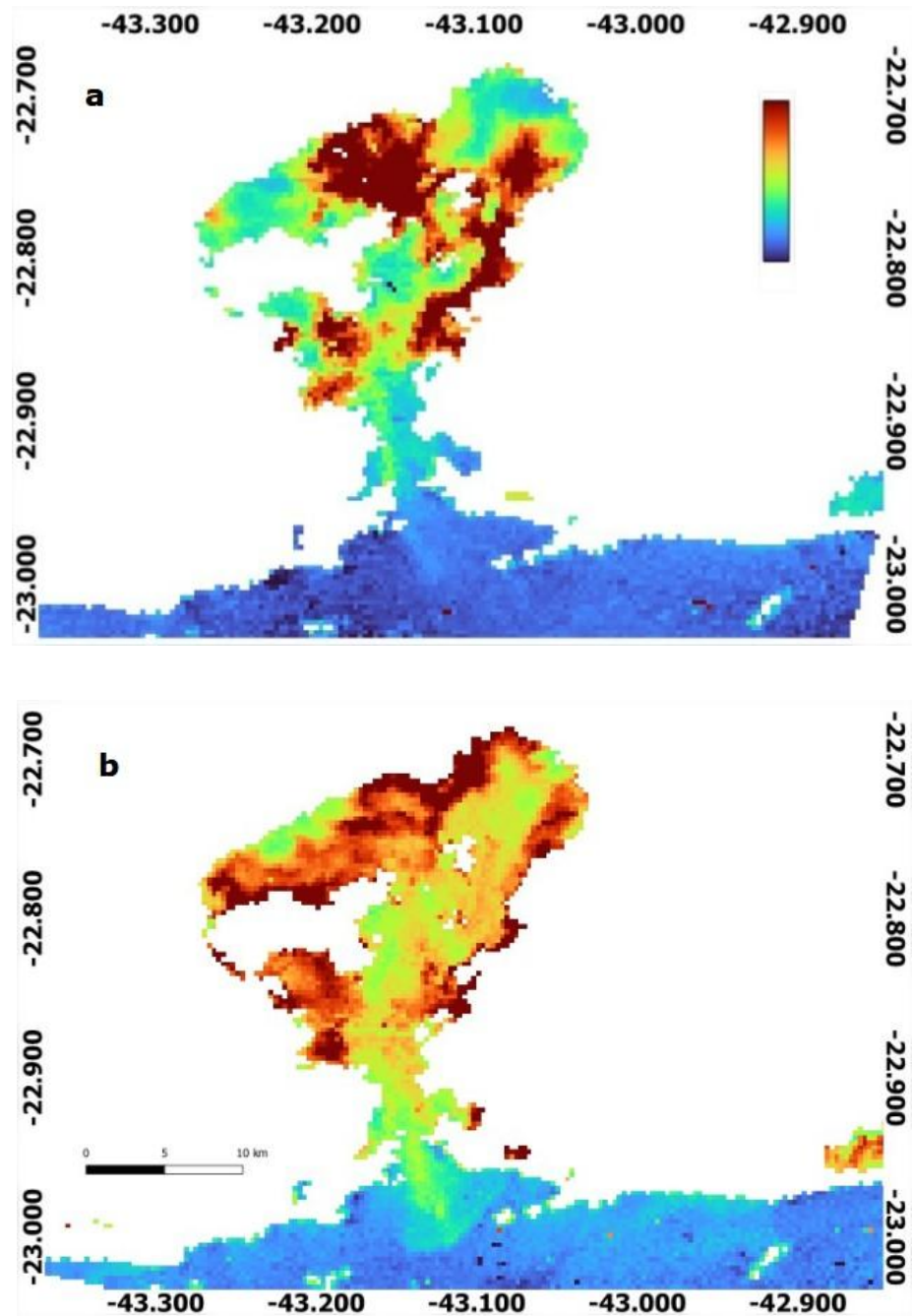
Figure 8: False color images obtained by the application of the Rrs709/Rrs674 ratio during phytoplankton blooms in Guanabara Bay on (a) March 17th, 2022 and (b) March 24th, 2022. Color gradients represent lower Rrs709/Rrs674 values in blue and higher Rrs709/Rrs674 in red.

The equation [Chl]=152.006*(Rrs709/Rrs674)-111.276 obtained by the best-fit curve analysis (Figure 4e - Table 6) was then applied on the March 24 2022 scene to generate a chlorophyll-a distribution map (Figure 9).
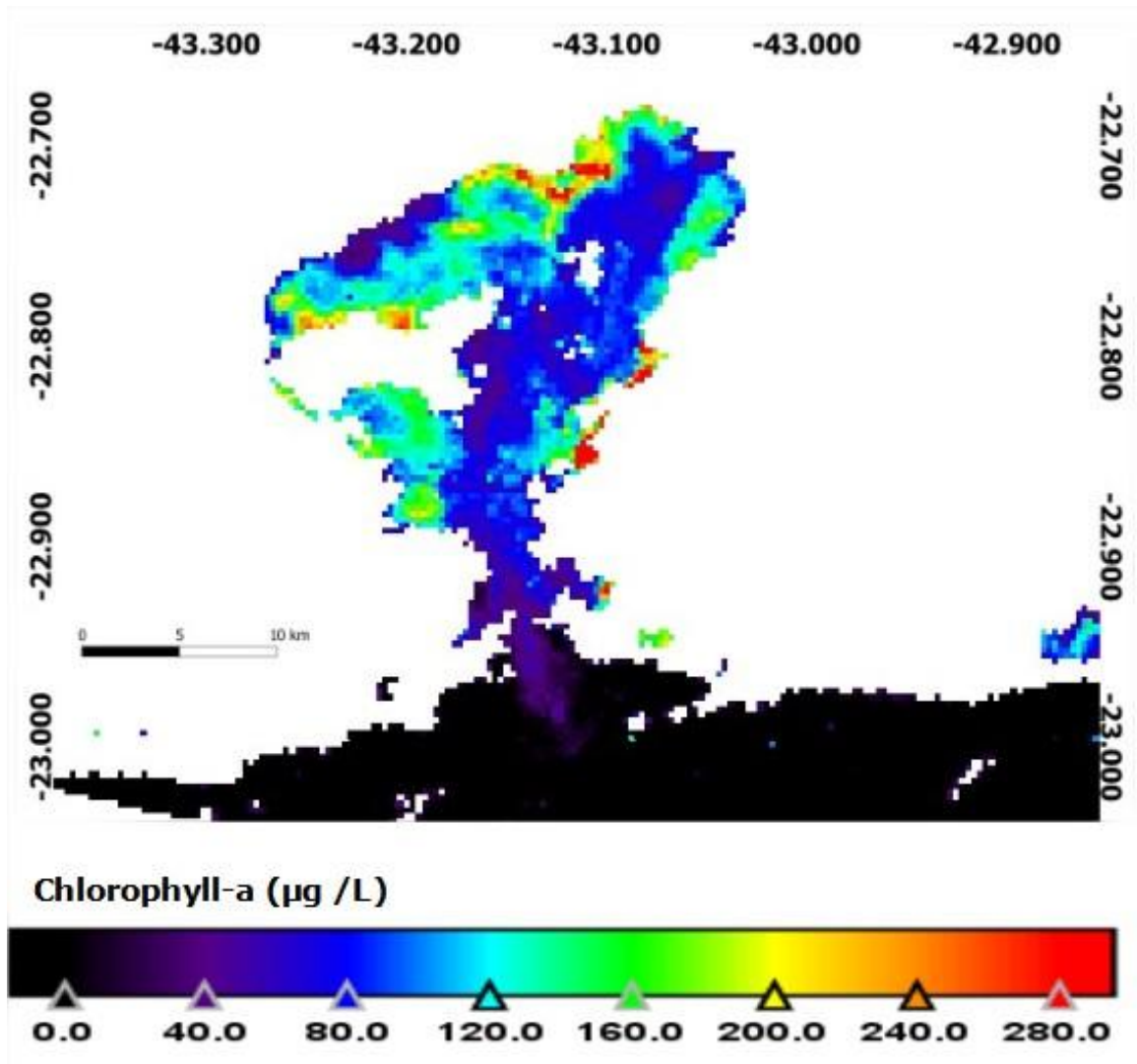
Figure 9: Chlorophyll-a distribution in Guanabara Bay for the March 24th, 2022 scene as an output of the Rrs709/Rrs674 model.

The chlorophyll-a distribution image indicates concentration values of 80 - 120 µg/L in the central channel and up to 280 µg/L in the areas with more constrained water circulation (with intense gradients being noted on the western section). This behavior is diagnostic of a generalized bloom situation that is coherent with the variation amplitude of chlorophyll concentration considering the *in-situ* dataset (Table 3) and also the results found on previous publications (Table 5). The notable gradients and the more frequent and intense colors of green and red in the region located

towards the bay's interior (Figure 9) corroborates with the fact that this area is more influenced by river discharge and therefore is more prone to parameter variability (due to its non uniform hydrodynamic characteristics) and biomass peaks (given a higher concentration of nutrients). Also, the western section where the color palette (Figure 9) indicates a greater frequency of chlorophyll-a values above 100 μg/L is known as the more critical region of the bay in terms of water quality (Paranhos et al., 2001; Lima, 2006). Taken together, these results emphasize the applicability of the formulation Rrs709/Rrs674 for phytoplankton bloom identification and indicate that the linear expression derived from this ratio (Figure 4e - Table 6) is able to provide a rational chlorophyll-a distribution map of the study region.

The lack of representation of chlorophyll-a patterns in the region outside Guanabara Bay (i.e features that can be seen on the RGB images that are not adequately represented in the RED-NIR profiles - Figure 8 neither on the chlorophyll distribution map - Figure 9) is possibly the result of the absorption/attenuation of the chlorophyll fluorescence signal by water (which is reasonable considering the lower phytoplankton abundance in this region and presumably the more disperse state of the cells that in this case would be located predominantly below the surface) and suggest the joint interpretation of RGB and RED-NIR proxy images for a more integrated phytoplankton bloom monitoring that contemplates the Guanabara Bay's interior and the adjacent areas, including the regions near Barra da Tijuca (approx -23.05, -43.42) and Itaipuaçu (approx -23.00, -42.90). This type of monitoring could provide short and long term information about changes in water quality and ecological status given the connection and fast response of phytoplankton to eutrophication (Coutinho et al., 2012; Hatherly, 2013) and extreme weather events as heat waves (Huang et al., 2018) and rainfalls (Yang et al., 2016; Jovanovic et al., 2017).

The implementation of a satellite based monitoring program in Guanabara Bay can be considered both important and challenging given the ecological and touristic importance of this region associated with the optical complexity of its waters. With approximately 384 km² of superficial area the bay shows a high degree of biological and physico-chemical variation and also areas with different levels of dynamics in respect of water circulation/tidal action which could promote different aggregation states of the phytoplankton cells. Nevertheless, the results obtained here shows the suitability of Sentinel-3 Red-NIR bands for chlorophyll-a retrieval and phytoplankton bloom monitoring in Guanabara Bay, which encourages further studies and prospects the near-future implementation of the Sentinel-3 program for a highly desirable integrated coastal resource management program in the state of Rio de Janeiro.

4. Conclusion and perspectives

The results shown in this work demonstrate the good statistical performance of six different Sentinel-3 RED-NIR algorithms for the analysis of phytoplankton biomass distribution in Guanabara Bay. The applied methodology outlined the distinct and somehow complementary responses obtained by two formulations: Rrs709/Rrs681 and Rrs709/Rrs674. This suggests that in the future, parallelly to the acquisition of additional *in-situ* chlorophyll-a data that should be used on a validation/cross validation process (serving as a measure of the models prediction ability) a switch algorithm shall be investigated (Smith et al., 2018; Lange et al., 2020).

Furthermore, it was observed that the Rrs709/Rrs674 ratio provided a concise representation of a complex bloom event in Guanabara Bay,

which reinforces the suitability of the ACOLITE atmospheric correction method for the study of complex waters (Vanhellemont and Ruddick, 2021) and indicates that this ratio could be used as a proxy for monitoring phytoplankton blooms in regions where *in-situ* chlorophyll data may be absent.

The results obtained by the RED-NIR bands support and incentivizes the utilization of Sentinel-3 data to develop a integrated ecological monitoring platform focusing in Guanabara Bay, where ideally remote sensing information, hydrometeorological data and also results derived from water quality stations located along the bay's drainage basins should be evaluated jointly and associated with actions that promote environmental education and social development to the local community.

Lastly, further efforts should be made to develop a chlorophyll-a time series that could trace the relationship between Guanabara Bay's phytoplankton biomass distribution and seasonal trends like monthly precipitation and heat waves, which are frequently intrinsically associated with the large scale phenomena El Niño and La Niña (Racaut et al., 2017; Zhong et al., 2022).

5. References

Ahmad A, Hashim N, Nordin L., (2009). Red Tide Detection Using Remotely sensed data: A Case Study of Sabah, Malaysia. Geografia OnlineTM Malaysian Journal of Society and Space. 5(3), 1-7.

Andrade, VS. (2018). Análise de hidrodinâmica ambiental e de qualidade de água na Baía de Guanabara via modelagem computacional. UFRJ-COPPE. Rio de Janeiro. Dissertação de Mestrado.

Binding, C., Greenberg, T., Jerome, J., Bukata, R.,and Letourneau, G., (2011). An assessment of MERIS algal products during an intense bloom in Lake of the Woods. Journal of Plankton Research. 33(5), 793–806. doi:10.1093/plankt/fbq133.

Binding, C.E., Greenberg, T.A., Bukata, R.P., (2013). The MERIS Maximum Chlorophyll Index; its merits and limitations for inland water algal bloom monitoring. J. Great Lakes Res. 39, 100–107. doi: 10.1016/j.jglr.2013.04.005.

Coutinho, M. T. P., Brito, A. C., Pereira, P., Gonçalves, A. S., Moita, M. T. (2012). A phytoplankton tool for water quality assessment in semi-enclosed coastal lagoons: Open vs closed regimes. *Estuarine, Coastal and Shelf Science*. 110, 134-146. doi:10.1016/j.ecss.2012.04.007

Cruz, A. A. A. D. (2016). Eutrofização antropogênica da Baía de Guanabara (Dissertação de mestrado, Universidade de Lisboa), 49 pp.

Dai Y., Yang S., Zhao D., Hu C., Xu W., Anderson D. M., Li Y., Song X.P. , Boyce D.G. , Gibson L., Zheng C., Feng L. (2023). Coastal phytoplankton blooms expand and intensify in the 21st century. Nature.615(7951), 280-284. doi: 10.1038/s41586-023-05760-y.

EUMETSAT (2018). Sentinel-3 OLCI Marine User Handbook. EUM/OPS-SEN3/MAN/17/907205, 41 pp.

Fistarol, G. O., Coutinho, F. H., Moreira, A. P. B., Venas, T., Cánovas, A., de Paula Jr., S. E. M., Coutinho, R., Moura, R. L., Valentin, J. L., Tenenbaum, D. R., Paranhos, R., do Valle, R. A. B., Vicente, A. C. P., Amado Filho, G. M., Pereira, R. C., Kruger, R., Rezende, C. E., Thompson, C. C., Salomon, P. S., Thompson, F. L. (2015)., Environmental and Sanitary Conditions of Guanabara Bay, Rio de Janeiro. *Front. Microbiol.* 6, 1232. doi:10.3389/fmicb.2015.01232.

Franz, G., Garcia, C. A., Pereira, J., de Freitas Assad, L. P., Rollnic, M., Garbossa, L. H. P., ... & Polejack, A., (2021). Coastal ocean observing and modeling systems in Brazil: initiatives and future perspectives. Frontiers in

Marine Science. 8, 681619. doi:10.3389/fmars.2021.681619

Fries, A. S., Coimbra, J. P., Nemazie, D. A., Summers, R. M., Azevedo, J. P. S., Filoso, S., Dennison, W. C., (2019). Guanabara Bay ecosystem health report card: Science, management, and governance implications. *Regional Studies in Marine Science*. *25*, 100474. doi:10.1016/j.rsma.2018.100474.

Giannini, F., Garcia, C.A.E., Tavano, V.M., Ciotti, A.M., (2013). Effects of low-salinity and high-turbidity waters on empirical ocean colour algorithms: an example for south western Atlantic waters. Cont. Shelf Res. 59, 84–96. doi:10.1016/j.csr.2013.04.013.

Gilerson, A.A., Gitelson, A.A., Zhou, J., Gurlin, D., Moses, W., Ioannou, I., Ahmed, S.A., (2010). Algorithms for remote estimation of chlorophyll-a in coastal and inland waters using red and near infrared bands. Optics Express. 18 (23), 24109–24125

Gin, K.Y.H., S.T. Koh, I.I. Lin, and E.S. Chan., (2002). Application of spectral signatures and colour ratios to estimate chlorophyll in Singapore's coastal waters. Estuarine. Coastal and Shelf Science. 55(5), 719-728.

Gitelson, A. (1992). The peak near 700 nm on radiance spectra of algae and water: relationships of its magnitude and position with chlorophyll concentration. International Journal of Remote Sensing 13(17), 3367–3373

Gitelson, A. A., Schalles, J. F., & Hladik, C. M., (2007). Remote chlorophyll-a retrieval in turbid, productive estuaries: Chesapeake Bay case study. *Remote Sensing of Environment*, *109*(4), 464-472. doi: 10.1016/j.rse.2007.01.016.

Gordon, H. R., Brown, O. B., Evans, R. H., Brown, J. W., Smith, R. C., Baker, K. S., et al. (1988). A semianalytic radiance model of ocean color. Journal of Geophysical Research. 93, 10909-10924. doi: 10.1029/JD093iD09p10909

Gower J., King S. Goncalves P., (2008) Global monitoring of plankton blooms using MERIS MCI, International Journal of Remote Sensing, 29:21, 6209-6216, doi: 10.1080/01431160802178110.

Gregoracci, G. B., Nascimento, J. R., Cabral, A. S., Paranhos, R., Valentin, J. L.,Thompson, C. C., (2012). Structuring of bacterioplankton diversity in a large tropical bay. *PLoS ONE.* 7, e31408. doi: 10.1371/journal.pone.0031408.

Gurlin, D., A.A. Gitelson, and W.J. Moses., (2011). Remote estimation of chl-a concentration in turbid productive waters — Return to a simple two-band NIR-red model? Remote Sensing of Environment. 115, 3479-3490. doi: 10.1016/j.rse.2011.08.011.

Ha, N. T. T., Thao, N. T. P., Koike, K., & Nhuan, M. T., (2017). Selecting the best band ratio to estimate chlorophyll-a concentration in a tropical freshwater lake using sentinel 2A images from a case study of Lake Ba Be (Northern Vietnam). *ISPRS International Journal of Geo-Information*. *6*(9), 290. doi:10.3390/ijgi6090290.

Hatherly, M. M. F. (2013). Alterações na estrutura da comunidade do microplâncton da Baía de Guanabara (RJ): 20 anos de amostragem. Universidade Federal do Rio de Janeiro (UFRJ). Dissertação de mestrado, 46 pp.

Huang, Q., Li, N. & Li, Y., (2021). Long-term trend of heat waves and potential effects on phytoplankton blooms in Lake Qiandaohu, a key drinking water reservoir. *Environ Sci Pollut Res.* 28, 68448–68459. doi: 10.1007/s11356-021-15414-z

IBGE – INSTITUTO BRASILEIRO DE GEOGRAFIA E ESTATÍSTICA . Censo Brasileiro de 2022. Rio de Janeiro: IBGE, 2023.

INMET, Instituto Nacional de Meteorologia. BDMEP - Banco de Dados Meteorológicos para Ensino e Pesquisa. Available at: https://g1.globo.com/rj/rio-de-janeiro/noticia/2022/03/09/rio-tem-o-marco-mais-quente-dos-ultimos-10-anos.ghtml Acessed in 05/29/2023

IOCCG (2019). Uncertainties in Ocean Colour Remote Sensing. (ed. Mélin F.) Dartmouth, NS, Canada, International Ocean-Colour Coordinating Group (IOCCG), 164pp. (Reports of the International Ocean-Colour Coordinating Group, No. 18). doi: 10.25607/OBP-696

IOCCG (2021). Observation of Harmful Algal Blooms with Ocean Colour Radiometry. (eds. Bernard, S., Kudela, R., Robertson Lain, L. and Pitcher, G.C.). Dartmouth, NS, Canada, International Ocean-Colour Coordinating Group (IOCCG), 165pp. (Reports of the International Ocean-Colour Coordinating Group, No. 20). doi: 10.25607/OBP-1042

Jovanović, J., Trbojević, I., Simić, G. S., Popović, S., Predojević, D., Blagojević, A., & Karadžić, V., (2017). The effect of meteorological and chemical parameters on summer phytoplankton assemblages in an urban recreational lake. *Knowledge & Management of Aquatic Ecosystems*. 418, 48. doi:10.1051/kmae/2017038

Jiao, H., Y. Zha, J. Gao, Y. Li, Y. Wei and J. Huang. (2006). Estimation of chlorophyll-a concentration in Lake Tai, China using in situ hyperspectral data. International Journal of RemoteSensing. 27(19), 4267-4276.

Kirk, J. T. (1994). *Light and photosynthesis in aquatic ecosystems*. Cambridge university press, 530 pp.

Kjerfve, B., Ribeiro, C. H., Dias, G. T., Filippo, A. M., & Quaresma, V. D. S.

(1997). Oceanographic characteristics of an impacted coastal bay: Baía de Guanabara, Rio de Janeiro, Brazil. *Continental shelf research*. *17*(13), 1609-1643. doi:10.1016/S0278-4343(97)00028-9.

Klemas, V., Weatherbee O., Field R., Xiao-Hai, Y. (2011). Remote sensing techniques for studying coastal ecosystems: an overview. Journal of Coastal Research. 27(1), 2–17.

Koponen, S., Attila, J., Pulliainen, J., Kallio, K., Pyhalahti, ¨ T., Lindfors, A., Rasmus, K., Hallikainen, M. (2007). A case study of airborne and satellite remote sensing of a spring bloom event in the Gulf of Finland. Continental Shelf Research. 27 (2), 228–244. doi:10.1016/j.csr.2006.10.006.

Lange PK, Jeremy Werdell P, Erickson ZK, Dall'Olmo G, Brewin RJW, Zubkov MV, Tarran GA, Bouman HA, Slade WH, Craig SE, Poulton NJ, Bracher A, Lomas MW, Cetinić I., (2020) Radiometric approach for the detection of picophytoplankton assemblages across oceanic fronts. Opt Express. 28(18), 25682-25705. doi: 10.1364/OE.398127.

Lima, E. C. (2006). Qualidade de água da Baía de Guanabara e Saneamento: Uma abordagem sistêmica. Universidade Federal do Rio de Janeiro (UFRJ). Tese de doutorado, 182 pp.

Lins, R. C., Martinez, J. M., Motta Marques, D. D., Cirilo, J. A., & Fragoso, C. R. (2017). Assessment of chlorophyll-a remote sensing algorithms in a productive tropical estuarine-lagoon system. *Remote Sensing*. *9*(6), 516, 1-19. doi: 10.3390/rs9060516

Liu B., D'Sa E. J., Maiti K., Rivera-Monroy V. H., Xue Z., (2021). Biogeographical trends in phytoplankton community size structure using adaptive sentinel 3-OLCI chlorophyll a and spectral empirical orthogonal functions in the estuarine-shelf waters of the northern Gulf of Mexico. Remote Sensing of Environment. 252, 112154. doi: 10.1016/j.rse.2020.112154

Mayr, L. M., Tenenbaum, D. R., Villac, M. C., Paranhos, R., Nogueira, C. R., Bonecker, S. L., & Bonecker, A. C. T., (1989). Hydrobiological characterization of Guanabara bay. ASCE. 124-138.

Mishra, S., Mishra, D.R.(2012). Normalized difference chlorophyll index: a novel model for remote estimation of chlorophyll-a concentration in turbid productive waters. Remote Sens. Environ. 117, 394–406. doi: 10.1016/j.rse.2011.10.016

Mollaee, S. (2018). Estimation of phytoplankton chlorophyll-a concentration in the western basin of Lake Erie using Sentinel-2 and Sentinel-3 data. *University of Waterloo. Master's thesis*, 80 pp.

Moses, W. J., Gitelson, A. A., Berdnikov, S., & Povazhnyy, V., (2009a).

Estimation of chlorophyll-a concentration in case II waters using MODIS and MERIS data—successes and challenges. *Environmental research letters*. *4(4)*, 1748- 9326. doi:10.1088/1748-9326/4/4/045005

Moses W. J., Gitelson A. A., Berdnikov S., Povazhnyy V. (2009b). "Satellite Estimation of Chlorophyll-a Concentration Using the Red and NIR Bands of MERIS - The Azov Sea Case Study,". *IEEE Geoscience and Remote Sensing Letters*. 6(4), 845-849. doi: 10.1109/LGRS.2009.2026657.

O'Reilly, J. E., Maritorena, S., Mitchell, B. G., Siegel, D. A., Carder, K. L., Garver, S. A., Kahru, M. & McClain, C. (1998). Ocean color chlorophyll algorithms for SeaWiFS. *Journal of Geophysical Research.* 103, 24937-24953. doi:10.1029/98JC02160

Oliveira, E. N., Fernandes, A. M., Kampel, M., Cordeiro, R. C., Brandini, N., Vinzon, S. B., Grassi, R. M., Pinto, F. N., Fillipo, A. M. & Paranhos, R., (2016). Assessment of remotely sensed chlorophyll-a concentration in Guanabara Bay, Brazil. *Journal of Applied Remote Sensing*. *10*(2), 026003. doi:10.1117/1.JRS.10.026003.

Paranhos, R., Andrade, L., Mendonça-Hagler, L. C., and Pfeiffer, W. C., (2001). Coupling bacterial density with activity in a tropical polluted coastal bay. Oecologia *Brasiliensis*. 9, 117–132. doi: 10.4257/oeco.2001.0901.09

Pirasteh S, Mollaee S., Fatholahi S. N., Li J. (2020) Estimation of Phytoplankton Chlorophyll-a Concentrations in the Western Basin of Lake Erie Using Sentinel-2 and Sentinel-3 Data, Canadian Journal of Remote Sensing. 46(5), 585-602. doi: 10.1080/07038992.2020.1823825

Pita, I. I C., (2019) Modelagem da Circulação em eventos Subinerciais na Baía de Guanabara-RJ. Dissertação de mestrado, 72 pp.

Racault, M.-F., Sathyendranath, S., Brewin, R.J.W., Raitsos, D.E., Jackson, T., Platt, T., (2017). Impact of El Nino variability on oceanic phytoplankton. Front. Mar. Sci. 4, 133. doi: 10.3389/fmars.2017.00133

Reguera, B., Escalera, L., Pazos, Y., Moroño, A. (2008). Episodios de fitoplancton tóxico en la Ría de Vigo. In: González-Garcés, A., Vilas-Martín, F., Álvarez-Salgado, X. (Eds.), La Ría de Vigo, una aproximación integral al ecosistema marino de la Ría de Vigo. Instituto de Estudios Vigueses, pp. 153–199.

Rodrigues, G.; Potes, M.; Penha, A.M.; Costa, M.J.; Morais, M.M., (2022). The Use of Sentinel-3/OLCI for Monitoring the Water Quality and Optical Water Types in the Largest Portuguese Reservoir. *Remote Sens. 14*, 2172. doi:10.3390/rs14092172.

Rumyantseva, A., Henson, S., Martin, A., Thompson, A.F., Damerell, G.M.,

Kaiser, J.,Heywood, K.J. (2019). Phytoplankton spring bloom initiation: the impact of atmospheric forcing and light in the temperate North Atlantic Ocean. Prog. Oceanogr. 178, 102202. doi: 10.1016/j.pocean.2019.102202

Rustamov, R. B., Hasanova, S., & Zeynalova, M. H., (2018). *Multi-purposeful application of geospatial data*. Intech. doi: 10.5772/intechopen.69713

Sampaio, M., (2003). Estudo de Circulação Hidrodinâmica 3D e Trocas de Massas D'água da Baía de Guanabara–RJ. Universidade Federal do Rio de Janeiro (UFRJ). Dissertação de mestrado, 213 pp.

Santos, S. J. D. C., (2015). Determinação do estado trófico a partir da aplicação dos índices O'Boyle e TRIX nos compartimentos da Baía de Guanabara, RJ. Universidade Federal Fluminense (UFF). Dissertação de mestrado, 100 pp

SEA/UEPSAM (2016). Diagnóstico do Estado da Baía de Guanabara (Programa de fortalecimento da governança e da gestão da Baía de Guanabara). KCI Technologies, Inc. 496 pp.

Shaik, I.; Mohammad, S.; Nagamani, P.V.; Begum, S.K.; Kayet, N.; Varaprasad, D., (2021). Assessment of chlorophyll-a retrieval algorithms over Kakinada and Yanam turbid coastal waters along east coast of India using Sentinel-3A OLCI and Sentinel-2A MSI sensors. Remote Sens. Appl. Soc. Environ. 24, 100644.

Silva, G. S. D. M., Garcia, C. A. E., (2021). Evaluation of ocean chlorophyll-a remote sensing algorithms using in situ fluorescence data in Southern Brazilian Coastal Waters. *Ocean and Coastal Research*. *69*. doi:10.1590/2675-2824069.20-014gsdms

Smith, M.E., Robertson Lain, L., Bernard, S., (2018). An optimized Chlorophyll a switching algorithm for MERIS and OLCI in phytoplankton-dominated waters. Remote Sens. Environ. 215, 217–227. doi: 10.1016/j.rse.2018.06.002.

Soares, F. S., de Mello, G. V., Neto, J. A. B., de Barros, R. S., Cruz, C. B. M., (2017) Classificação das águas da Baía de Guanabara utilizando o sensor OLI/Landsat 8. Anais do 15° Simpósio Brasileiro de Sensoriamento Remoto. 2091-2098.

Tao B., Mao Z., Pan D., Shen Y., Zhu Q., Chen J., (2013). Influence of bio-optical parameter variability on the reflectance peak position in the red band of algal bloom waters,Ecological Informatics. 16, 17-24. doi: 10.1016/j.ecoinf.2013.04.005.

Tenório, M. M. B., Le Borgne, R., Rodier, M., & Neveux, J., (2005). The impact of terrigenous inputs on the Bay of Ouinné (New Caledonia)

phytoplankton communities: a spectrofluorometric and microscopic approach. *Estuarine, Coastal and Shelf Science*. *64*(2-3), 531-545. doi:10.1016/j.ecss.2005.02.030.

Tran, M.D.; Vantrepotte, V.; Loisel, H.; Oliveira, E.N.; Tran, K.T.; Jorge, D.; Mériaux, X.; Paranhos, R., (2023). Band Ratios Combination for Estimating Chlorophyll-a from Sentinel-2 and Sentinel-3 in Coastal Waters. *Remote Sens. 15*, 1653. doi:10.3390/rs15061653

Vanhellemont, Q., Ruddick, K, (2016). Acolite for Sentinel-2: Aquatic applications of MSI imagery. In Proceedings of the 2016 ESA Living Planet Symposium, Prague, Czech Republic. 9–13.

Vanhellemont, Q.; Ruddick, K. (2018). Atmospheric correction of metre-scale optical satellite data for inland and coastal water applications. Remote Sens. Environ. 216, 586–597. doi: 10.1016/j.rse.2019.03.010

Vanhellemont, Q. (2019). Adaptation of the dark spectrum fitting atmospheric correction for aquatic applications of the Landsat and Sentinel-2 archives. Remote Sens. Environ. 225, 175–192.

Vanhellemont, Q. and Ruddick, k. (2021). Atmospheric correction of Sentinel-3/OLCI data for mapping of suspended particulate matter and chlorophyll-a concentration in Belgian turbid coastal waters. Remote Sensing of Environment. 256, 112284. doi: 10.1016/j.rse.2021.112284.

Vermote, E. F., Roger, J. C., Ray, J. P. (2015). *MODIS Surface Reflectance User 's Guide*. Collection 6, 34 pp.

Villac, M. C., Tenenbaum, D. R (2010). The phytoplankton of Guanabara Bay, Brazil. I. Historical account of its biodiversity. *Biota Neotrop*. 10 (2), 271-293. doi: 10.1590/S1676-06032010000200030.

Wang, M., Shi. W, Jiang, L. (2012). Atmospheric correction using near-infrared bands for Satellite Ocean color data processing in the turbid western Pacific region. OSA publishing, Optics Express. 20, 741–753. doi: 10.1364/OE.20.000741.

Watanabe, F. S. Y., Alcântara, E., & Stech, J. L. (2018). High performance of chlorophyll-a prediction algorithms based on simulated OLCI Sentinel-3A bands in cyanobacteria-dominated inland waters. *Advances in Space Research*. 62(2), 265-273. doi:10.1016/j.asr.2018.04.024.

Yang, H.; Kong, J.; Hu, H.; Du, Y.; Gao, M.; Chen, F. (2022). A Review of Remote Sensing for Water Quality Retrieval: Progress and Challenges. *Remote Sens. 14*, 1770. doi:10.3390/rs14081770.

Yang Z, Zhang M, Shi X, Kong F, Ma R, Yu Y. (2016). Nutrient reduction magnifies the impact of extreme weather on cyanobacterial bloom

formation in large shallow Lake Taihu (China). Water Res. 103, 302–310.

Zeng, C.; Binding, C. (2019). The Effect of Mineral Sediments on Satellite Chlorophyll-a Retrievals from Line-Height Algorithms Using Red and Near-Infrared Bands. *Remote Sens. 11*, 2306. doi:10.3390/rs11192306

Zhong, Y., Laws, E. A., Zhuang, J., Wang, J., Wang, P., Zhang, C., et al. (2022). Responses of phytoplankton communities driven by differences of source water intrusions in the El niño and la niña events in the Taiwan strait during the early spring. Front. Mar. Sci. 9, 997591. doi: 10.3389/fmars.2022.997591.

Zhou M., Wu M.,Zhao L.,Zheng L., Li B., (2021). Temporal and Spatial Distributions and Influencing Factors of HABs Outbreaks around the North of Shandong Peninsula during 2000–2019: Based on Remote Sensing Images and Field Monitoring Data. Geocarto International. 37, 1-14. doi: 10.1080/10106049.2021.2002425.